GDCh

Research Article

Angewandte
Chemie
International Edition
www.angewandte.org

Diboriranes

π-Complexes Derived from Non-classical Diboriranes: Side-on vs. End-on Carbonylative Ring Expansion

Philipp Grewelinger, Carsten Präsang, Michael Zimmer, Bernd Morgenstern, and David Scheschkewitz*

Abstract: Unlike cyclopropanes, the analogous B_2C species (diboriranes) tend to adopt non-classical Hückel-aromatic structures with bridging moieties R between the boron atoms. The coordination of the thus generated cyclic $2e^-$ π-system to transition metals is completely unexplored. We here report that complexation of non-classical diboriranes cyclo-μ-RB_2Dur_2CPh (R=H, $SnMe_3$; Dur = 2,3,5,6-tetramethylphenyl) to $Fe(CO)_3$ fragments allows for the carbonylative ring expansion of the B_2C ring to either four- or five-membered rings depending on the nature of the BRB 3-center-2-electron bond (3c2e): The H-bridged diborirane (R=H) initially reacts with $Fe_2(CO)_9$ to the allylic π-complex with an agostic BH/Fe interaction. Subsequent formal hydroboration of CO from excess $Fe_2(CO)_9$ results in the side-on ring expansion under formation of a five-membered B_2C_2O ring, coordinated to the $Fe(CO)_3$ moiety. In contrast, in case of the stannyl-bridged diborirane (R=$SnMe_3$) under the same conditions, CO is added end-on to the B–B bond with the carbon terminus formally inserting into the B_2Sn 3c2e-bond. The two carbonylative ring expansion products can also be described as *nido* and *closo* clusters, respectively, according to the Wade-Mingos rules.

Introduction

Organometallic transition metal species are of tremendous importance in organic and inorganic chemistry, first and foremost as catalysts but also as structure-determining motifs[1] and functional groups[2,3] in materials. Aromatic π-coordinating ligands such as benzene, cyclopentadienide and related have been at the forefront of the field during the past 60 years. The coordination chemistry of boron containing aromatic heterocycles such as diboretes,[4] borolediides,[5] bora- and boratabenzenes[6] and borepins[7] is similarly dominated by the donation of the π-system toward the electron deficient metal center. In contrast, transition metal complexes of three-membered aromatic boracycles are even scarcer than those of the isoelectronic cyclopropenium cations.[8] For instance, the first and still only triborirandiide was obtained by Braunschweig et al. as a dimer with inverse double-sandwich structure involving four sodium counter cations,[9] but its ligand properties toward transition metals remain unexplored. Similarly, despite the straightforward access to borirenes by borylene transfer to alkynes,[10] only a few borirene metal complexes have been reported. Apart from a borirene σ-complex,[11] there is only one example of a η^3-bonded π-complex, recently reported by Braunschweig and co-workers: the chromium carbonyl complex **I** (Scheme 1) is obtained in low yield as a side-product during the photolytic transfer of a bulky borylene from $Cr(CO)_5$ to tolane, PhCCPh.[12] Recently, we disclosed the straightforward synthesis of a non-classical diborirane and the corresponding anionic diboriranides **II** as well as first investigations into the coordination behavior of the latter.[13] Complexes **II** with the cationic metal centers M, exclusively bonded in σ-fashion to the perimeter of the anionic B_2C ring, were readily obtained by salt metathesis with the lithium salt. Apart from the reduction to the diboriranide, the reactivity of the neutral diborirane – containing a "non-classical" 3c2e σ-bond (BHB) – is completely unknown. According to DFT calculations, the Hückel-aromatic $2e^-$ π-system of neutral non-classical diboriranes constitutes the

[*] M. Sc. P. Grewelinger, Dr. C. Präsang, Dr. M. Zimmer,
Prof. Dr. D. Scheschkewitz
Krupp-Chair for General and Inorganic Chemistry,
Saarland University
66123 Saarbrücken, Germany
E-mail: scheschkewitz@mx.uni.saarland.de

Dr. B. Morgenstern
Service Center X-ray diffraction
Saarland University
66123 Saarbrücken, Germany
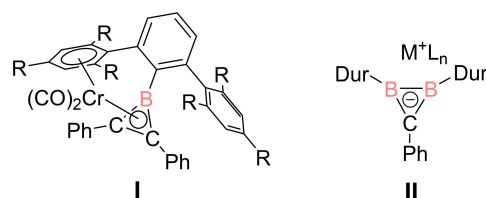
Scheme 1. Selected metal complexes of three-membered aromatic boracycles (I: R=^iPr; II: M^+L_n=Li(thf)$_2$, AuPPh$_3$, CuCuLi(thf)$_3$, ZnCl$_2$Li-(OEt)$_2$, SnMe$_3$, Dur = 2,3,5,6-Me$_4$C$_6$H).

highest occupied molecular orbital (HOMO) and should therefore be amenable to η^3-coordination.[13]

Here, we report the first π-complexes involving B_2C moieties that retain a certain – albeit weak – B–B interaction. The coordination to iron carbonyl fragments gives rise to subsequent carbonylative ring expansion. Depending on the nature of the B–B-bridge in the diborirane precursor this occurs either side-on or end-on to yield five- and four-membered ligand systems, respectively.

Results and Discussion

Synthesis of diborirane π-complexes

Quantum chemical calculations had shown that the HOMO of diborirane **1** is composed of the delocalized π-system of the B_2C ring.[13] We therefore anticipated it to be well suited as π-ligand for transition metals. In addition, the BHB bridge could support the coordination through its σ-electrons as BH bonds have been repeatedly employed as σ-donors to transition metal centers.[14] Inspired by the first diborane transition metal complexes as well as by Fehlner's borirene-containing Fe_3C_2B *closo* cluster,[15] we opted for an iron carbonyl as precursor.

The addition of 1.6 equivalents of $Fe_2(CO)_9$ to the non-classical diborirane **1** in benzene indeed results in a color change from colorless to red. After workup, the diborirane iron complex **2** is obtained as red crystals from hexane after 18 hours (Scheme 2). Upon heating the iron complex **2** to 150 °C for 1 h, the non-classical diborirane **1** is liberated as verified by multinuclear NMR spectroscopy (Scheme 2), which suggests that the diborirane coordination to the $Fe(CO)_3$ fragment is only moderately strong. For comparison, the addition of $Fe_2(CO)_9$ to the lithium salt of diboriranide **II** (M$^+$Ln=Li(thf)$_2$) does not lead to the uniform formation of a product, but only to an intractable product mixture underscoring the differences between the neutral diborirane **1** and the anionic diboriranide.

X-ray diffraction on a single crystal of **2** confirmed the coordination of the $Fe(CO)_3$ fragment above the B_2C moiety (Figure 1). The hydrogen atom has forfeited its bridging position between the two boron atoms and bridges B1 and Fe1 instead in an agostic interaction of the BH bond. Upon coordination to the iron center, the B1–B2 distance is widened significantly (**1**: 1.769 Å); **2**: 2.380(3) Å). The B–C–B angle (106.7(1)°), however, is more acute than in
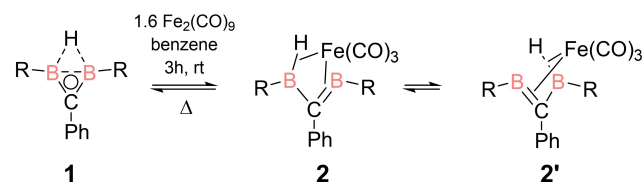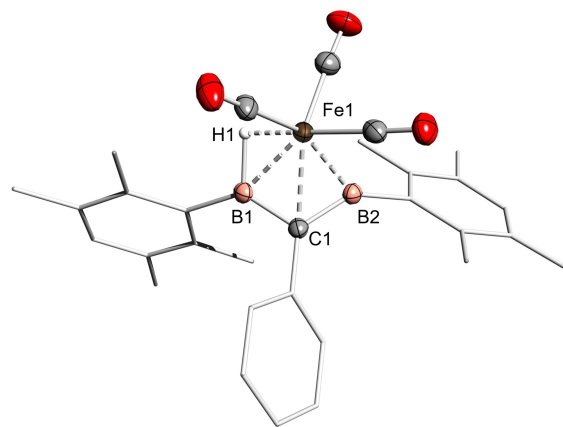
Figure 1. Molecular structure of diborirane iron complex **2** in the solid state. Thermal ellipsoids at 50 % probability. Selected bond lengths [Å] and angles [°]: B1–B2 2.380(3), B1–C1 1.498(2), B2–C1 1.496(2), B1–H1 1.296(2), B1–Fe1 2.150(2), B2–Fe1 2.038(2), Fe1–H1 1.61(2), C1–Fe1 2.137(2); B1–C1–B2 106.7(1).[19]

Berndt's borylmethyleneborane suggesting some remaining bonding interaction between the boron atoms in **2**.[16] Homodiborirane complexes reported by Siebert and Berndt also show larger B–C–B angles (132.3 to 150.3°) and B–B bond lengths (2.573 to 2.896 Å) than **2**.[17]

The elongation of the B–C$_{ring}$ bonds upon coordination is significantly more pronounced for B1–C1 than for B2–C1 (**1**: B1–C1 1.442(2) Å; B2–C1 1.442(2) Å; **2**: B1–C1 1.498(2) Å; B2–C1 1.469(2) Å), which is consistent with a certain B2–C1 double bond character (Scheme 2). In line with this assertion, the iron atom is located closer to B2 (B2–Fe1 2.038(2) Å) than to B1 (B1–Fe1 2.105(2) Å), presumably an effect of the stronger donation of the B=C π-bond compared to the BH σ-bond. The C1–Fe1 distance of 2.137(2) Å is similar to those in the aforementioned borirene-derived *closo* cluster[15] and in a methyleneborane iron complex reported by the Braunschweig group.[18] The BH distance in **2** (B1–H1 1.296(2) Å) remains almost unchanged from those of the bridging hydrogen of diborirane **1** (B1–H1 1.278(2) Å; B2–H1 1.309(2) Å) indicating a considerable agostic interaction with Fe1. Indeed, the Fe1–H1 bond of 1.61(2) Å is in the range of such bonds in reported borohydride iron complexes.[14h,i]

The ^{1}H NMR signal in the far high field at $\delta = -11.4$ ppm is attributed to the BH hydrogen. The broadening caused by the coupling to one quadrupolar boron nucleus confirms this assignment. Compared to non-classical diborirane **1**, the signal for the B-bonded hydrogen is exceptionally upfield shifted by $\Delta\delta = 18.7$ ppm, unambiguously proving its hydridic character due to agostic interactions with the iron fragment.[14c] The *ortho* and *meta* CH$_3$ groups of the duryl substituents each give rise to only one ^{1}H and ^{13}C NMR signal, which could either be due to a more symmetrical structure or rapid equilibration between the degenerate species **2** and **2'** in solution (Scheme 2). VT NMR did not help in discriminating between these two orthogonal explanations as even at -60 °C no splitting of the signals was observed.

Scheme 2. Synthesis of diborirane iron carbonyl complex **2** starting from non-classical diborirane **1** and the degenerate equilibrium in solution between **2** and **2'** involving 1,3-hydride migration (R=Dur=2,3,5,6-Me$_4$C$_6$H).

Consistent with above, the ^{11}B NMR spectrum of the diborirane complex **2** shows only one signal at δ = 68.4 ppm. In contrast, ^{11}B SPE/MAS NMR detects two distinct signals at δ = 85.1 ppm and 50.6 ppm in line with the two chemically inequivalent boron atoms in the solid state. The average of these chemical shifts of 67.5 ppm, however, is very close to the observed solution signal and thus provides a first indication of fluxionality in solution. DFT calculations at the BP86/def2SVP level further strengthen this interpretation: attempts to optimize a symmetrical geometry analogous to BHB-bridged diborirane **1** unequivocally led to relaxation to unsymmetrical **2** (Scheme 2). The GIAO-computed ^{11}B NMR shifts at δ = 79.5 and 44.5 ppm (B3LYP/def2tzvpp) are very close to the experimental signals in the solid state. While the boron atom associated to the downfield signal is slightly more shielded than in Braunschweig's methyleneborane iron complex,[18] the upfield shifted signal is in the range for σ-borane complexes.[14j] The alternative explanation of an inherently symmetrical structure in solution can be excluded as the signal for the ring carbon atom matches the one in the solid state ^{13}C CP/MAS spectrum. It is significantly upfield shifted compared to diborirane **1** (δ = 50.0 for **2** vs. 136.4 ppm for **1**) indicating little if any cyclic delocalization of the π-electrons across the B_2C ring.

The solid state IR spectrum of **2** shows three clear signals at 1967, 1986 and 2045 cm^{-1} (see SI). DFT calculations at the BP86/def2SVP level of theory give vibrations at 2004, 2013 and 2059 cm^{-1}, only slightly blue shifted compared to the experimental data. In hexane solution, two bands at 1990 and 2049 cm^{-1} in an approximate 2:1 ratio are observed suggesting rapid turnstile-like exchange of the CO positions in solution.[20] DFT calculations indicate the B–H stretching frequency at 1782 cm^{-1}, which, however, cannot be assigned due to its occurrence in the fingerprint area (see SI).

The longest wavelength absorption in the experimental UV/Vis spectrum of **2** (see SI) is observed as a very broad band at an estimated $λ_{max}$ of about 420 nm (ε = 1445 M^{-1} cm^{-1}) tailing to about 500 nm. A TD-DFT calculation at the B3LYP/def2tzvpp level of theory assigns the band to two weak transitions at 470 nm (HOMO→LUMO) and at 407 nm (HOMO−1→LUMO; see SI). The HOMO of complex **2** corresponds to the backdonation of an occupied d orbital at iron into the vacant σ-type p orbital at B2 of the B=C bond (Figure 2). The HOMO−1 reflects the bonding combination of the B_2C π-system (predominantly but not exclusively located at C1 and B2) and a vacant d orbital at the iron center. The LUMO is dominated by the vacant p orbital at hydrogen-bonded B1 with some minor contributions at the pending duryl groups and the iron center. The bonding interaction between the BH σ-bond and a d orbital at iron is identified at very low energy as HOMO−18 (see SI). Quantum theory of atoms in molecules (QTAIM, see SI) confirms the substantial weakening of the B–B interaction in **2** as no bond critical point is found between the boron atoms.

2

HOMO−1 (−6.18)	HOMO (−5.95)	LUMO (−2.22)

3

HOMO−3 (−6.23)	HOMO−1 (−6.18)	LUMO (−2.47)

5

HOMO−2 (−6.19)	HOMO (−5.77)	LUMO (−2.63)
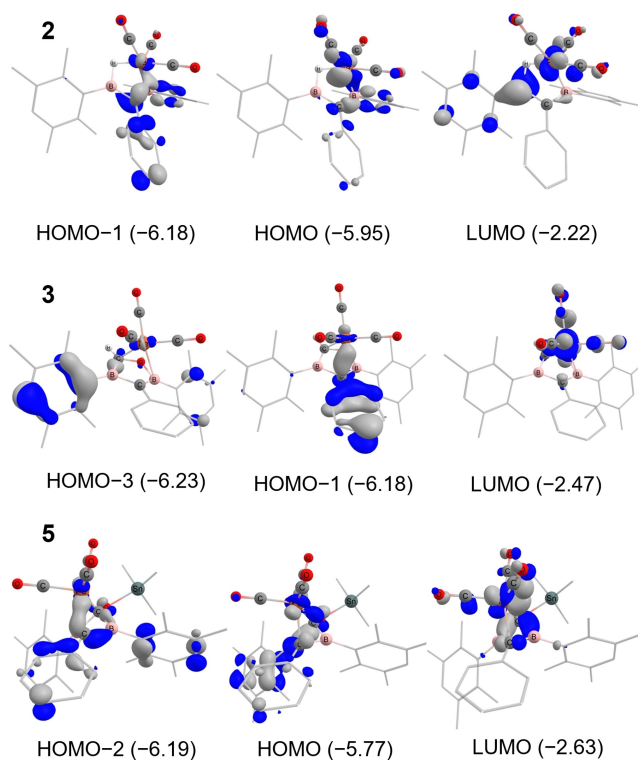
Figure 2. Selected frontier orbitals of iron complexes **2**, **3** and **5** (energy in eV, contour value = 0.06).

Carbonylative ring expansion

The interest in boron containing transition metal complexes is intimately related to their role in important catalytic processes[21] and hence to the activation of the C–B or BH bond for reactions with otherwise unreactive substrates. In view of the borylmethyleneborane nature of **2** with coordination of both the BH σ-bond and the B–C π-bond to the iron center, we envisaged the possibility of hydroboration of a small molecule such as carbon monoxide with iron complex **2**. While extended exposure of **2** to an excess of CO only results in the liberation of the free diborirane **1**, stirring of **2** with five equivalents $Fe_2(CO)_9$ in toluene for 72 h indeed leads to the formation of a new product as indicated by ^{1}H NMR monitoring.

Two singlets each for the *ortho* and *meta* CH_3 groups confirm the chemical inequivalence of the duryl substituents and hence a less symmetric structure. Consequently, the ^{11}B NMR spectrum also shows two signals for the boron atoms at δ = 26.2 ppm and 34.5 ppm and thus upfield-shifted signals compared to that of iron complex **2**. The similarity of the chemical shifts to those of 1,3-diborole metal complexes[22] suggests the constitution of **3**, the formal hydroboration product of **2** and one molecule of CO and hence the expansion of the diborirane to a five-membered ring (Scheme 3). Carbonylative ring expansions by transition metal carbonyls have been reported for various strained heterocycles,[23] but not for boron containing systems.
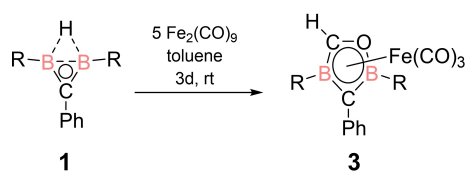
Scheme 3. Hydroboration of carbon monoxide with **1** to yield η^5-complex of five-membered diboracycle **3** (R=Dur=2,3,5,6-Me$_4$C$_6$H).

Due to the higher electronegativity of oxygen compared to carbon, the signal at $\delta = 34.5$ ppm is tentatively assigned to the oxygen-bonded boron atom. The ^{13}C NMR spectrum at 213 K shows two broad signals at $\delta = 109.0$ and 90.0 ppm which we attribute to the ring carbon atoms. The signal at $\delta = 109.0$ ppm, still in the aromatic region, is due to the B–C–B carbon atom. The significant downfield shift compared to the ring carbon in diborirane complex **2** ($\delta = 50.0$ ppm) confirms a more pronounced cyclic delocalization of the π-electrons. This gains further support from the ^{13}C NMR signal of the other endocyclic carbon signal at $\delta = 90.0$ ppm being substantially deshielded compared to Erker's saturated oxadiborolane NHC adduct **III** ($\delta = 77.4$ ppm, Scheme 4).[24]

The IR spectrum of the red solid shows two strong signals at 2000 cm^{-1} and 2059 cm^{-1} in the region for CO stretching modes. DFT calculations find CO vibrations at 2026, 2028 and 2079 cm^{-1} again slightly blue shifted compared to the experimental data. The significant blue-shift compared to diborirane complex **2** suggests weaker backbonding from the iron center to the CO π*-orbitals due to an increased charge transfer to the boron ligand. Incidentally, the CO stretching frequencies are very similar to those of Herberich's Fe(CO)$_3$-borole complex **IV** (Scheme 4).[25]

The η^5-complex **3** can also be obtained by adding 3.4 equivalents of Fe$_2$(CO)$_9$ to diborirane iron complex **2**, confirming its intermediacy. As the formal hydroboration product **3** cannot be obtained from isolated **2** by simple addition of 1 atm of CO gas, we assume an initial addition of an Fe$_x$(CO)$_y$ fragment of an unknown nature to **2** and subsequent transfer of a CO molecule. The spatially proximal B–H would then hydroborate a polarized CO bond. The liberated Fe$_x$(CO)$_y$ fragment could react with Fe$_2$(CO)$_9$ explaining that more than one equivalent of Fe$_2$(CO)$_9$ are required for full conversion. Free non-classical diborirane **1** does not react with CO either, which under-

scores the necessity of the presence of the unknown iron species.
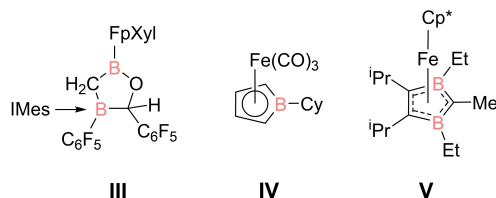
Crystallization from a concentrated hexane solution yields dark-red single crystals suitable for x-ray diffraction (Figure 3). The structure was solved in the triclinic space group P$\bar{1}$ and confirms the constitution of **3** as an 4-oxa-1,3-diborole ligand η^5-coordinated to the Fe(CO)$_3$ fragment in a piano-stool fashion. In accordance with the Wade-Mingos counting rules (16 skeletal electrons for six centers), the compound can equally be described as six-vertex *nido* cluster with a pentagonal-pyramidal polyhedron. The donation of the π-electrons to the iron fragment in **3** is more pronounced than in **2**, which is expressed in longer B–C bonds (**2**: B1–C1 1.498(2) Å, B2–C1 1.496(2) Å; **3**: B1–C1 1.544(2) Å; B2–C1 1.559(2) Å), albeit still shorter than typical B–C single bonds. The B2–C2 bond of **3** of 1.501(2) Å is shorter than the other two B–C bonds, which is probably a consequence of the much lower steric congestion at C2.

The five-membered ring in **3** adopts an envelope conformation with the phenyl-substituted C1 bent toward Fe1 (folding angle B1–C1–B2/B1–O1–C2–B2 22.1(1)°). This folding minimizes the steric interactions between the phenyl and the duryl substituents although it is less pronounced than in an iron sandwich complex with an anionic η^5-1,3-diborole ligand reported by Siebert et al. (**V** in Scheme 4; folding angle 41.3°).[22a] In any case, the bent structure appears to maximize the overlap between the B$_2$C$_2$O π-electrons and the d$_z^2$ orbital at the iron center in sight of considerable steric strain. Compared to Siebert's 1,3-diborole complex **V**, the boron-iron distances in **3** (B1–Fe1 2.299(2) Å; B2–Fe1 2.315(2) Å) are only slightly larger (**V**: 2.248 Å), while the iron contact of the folded carbon (**3**: C1–Fe1 2.175(2) Å) is substantially elongated (**V**: 1.899 Å). In turn, the other carbon-iron distance in **3** (C2–Fe1 2.025(2) Å) is significantly shorter (**V**: 2.116 Å).

Scheme 4. Reported five-membered diboracycle **III**[24] and complexes **IV**[25] and **V**[22a] (FpXyl = 2,5-bis(trifluoromethyl)phenyl; IMes=N,N'-dimesitylimidazolylidene; Cp* = pentamethylcyclopentadienyl).
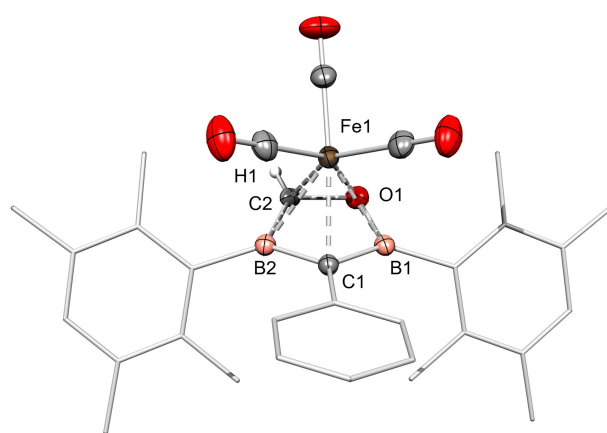
Figure 3. Molecular structure of formal hydroboration product **3** in the solid state. Thermal ellipsoids at 50% probability. Selected bond lengths [Å] and angles [°]: B1–C1 1.544(2), B2–C1 1.559(2), B1–O1 1.466(2), B2–C2 1.501(2), C2–O1 1.440(2), B1–Fe1 2.229(2), B2–Fe1 2.315(2), C1–Fe1 2.175(2), C2–Fe1 2.025(2); B1–C1–B2 106.3(1).

These observations can be rationalized with the canonical orbitals as calculated by DFT at the B3LYP/def2tzvpp level of theory (Figure 2) since the significant overlap of the rings π-system mainly located at C1 with the irons d orbital can be seen in the HOMO−1. The HOMO−3 is composed of the bonding combination of the lone pair at C2 and another d orbital of iron. The LUMO shows a vacant d orbital with antibonding combination of the COs π-system. The longest wavelength absorption in the experimental UV/Vis spectrum (see SI) at $\lambda_{max} = 403$ nm ($\varepsilon = 2450$ M^{-1} cm^{-1}) tails to around 500 nm in a similar manner as diborirane complex **2**. A TD-DFT calculation at the B3LYP/def2tzvpp level of theory assigns the band to the HOMO→LUMO transition at 401 nm.

Although certainly nowhere near as well developed as hydroboration, borostannylation has been reported as an effective tool for the cyclization of α,ω-dienes.[26] We were thus interested in the behavior of Me$_3$Sn-bridged diborirane **4**[13] toward Fe$_2$(CO)$_9$. As in the case of the non-classical diborirane **1**, DFT calculations showed that the HOMO of diborirane derivative **4** is composed of the B$_2$C rings π-system.[13] Indeed, the addition of 1.2 equivalents of Fe$_2$-(CO)$_9$ to the tin-bridged diborirane **4** in toluene leads to a color change of the reaction mixture from colorless to red-brown and the appearance of a uniform set of new signals in the ^{1}H NMR spectrum (Scheme 5). The product appears to be symmetrical in solution due to the presence of only one signal each for the *ortho* and *meta*-CH$_3$ groups of the duryl substituents. The single ^{11}B NMR signal at $\delta = -17.7$ ppm is considerably more shielded than in both **2** and **3**. While the ^{13}C NMR signal for the endocyclic Ph-substituted carbon atom ($\delta = 111.2$ ppm) is similar to the one in the five-membered ligand of complex **3** ($\delta = 109.0$ ppm), the oxygen-bonded ring carbon signal is dramatically downfield shifted to $\delta = 257.7$ ppm.

This carbon atom is thus considerably more deshielded than the COs at the iron center ($\delta = 211.6$ ppm). This is indicative of a small degree of backdonation from the iron center to the empty p orbital of the CO moiety. The ^{119}Sn NMR spectrum shows a signal at $\delta = 191.3$ ppm, downfield-shifted by $\Delta\delta = 230$ ppm compared to precursor **4** as expected for the reduction in coordination number at tin from five to four. The IR spectrum shows CO vibrations at similar wavenumbers as in diborirane complex **2** at 1966, 1983 and 2045 cm^{-1}. DFT calculated values at 1994, 2013 and 2059 cm^{-1} are once more slightly blue-shifted compared to the experimental data. Taken together, the analytical data is in line with the constitution of 1,3-dihydro-1,3-diborete complex **5**.
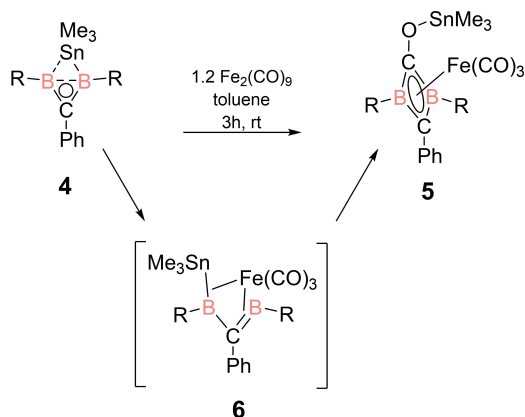
Dark red-brown crystals of **5** suitable for an x-ray diffraction analysis were obtained from a concentrated hexane solution at 0 °C (Figure 4). The crystal structure confirms the end-on insertion of one carbon monoxide ligand into the 3c2e BBSn bond to yield a four-membered 1,3-diborete ring system coordinated in η^4-fashion to the Fe(CO)$_3$ moiety. With a cluster electron count of 12, the compound can be described as a five-vertex *closo* cluster with an B$_2$C$_2$Fe scaffold and thus as a distorted trigonal bipyramid. As a consequence, the B$_2$C$_2$ moiety adopts a bicyclo(1.1.0)butane-like structure, which is, however, also familiar for free 1,3-diboretes.[27] The Fe(CO)$_3$ unit resides above this moiety, yet the boron atoms retain a considerable degree of mutual interaction as the B–B distance is elongated just moderately (B1–B2: 1.871(5) Å) compared to precursor **4** (B–B: 1.799 Å).[13] In Stone's ferracar-borates with FeCB$_7$ and Fe$_2$CB$_7$ scaffolds the distance between the two carbon-connected boron vertices are considerably expanded to 2.137 and 1.996 Å, respectively.[28] In fact, the B–B distance in **5** is significantly shorter than in a free 1,3-diborete (2.16 Å)[27] and slightly shorter than in 1,3-diborete nickel complex (1.890 Å), recently reported by Braunschweig and co-workers.[29]

The longest wavelength absorption in the experimental UV/Vis spectrum (see SI) is observed as a very broad band of low intensity at $\lambda_{max} = 600$ nm ($\varepsilon = 481$ M^{-1} cm^{-1}) tailing to around 650 nm. The TD-DFT calculated $\lambda_{max} = 620$ nm

Scheme 5. Complexation of tin bridged diborirane **4** to the four-membered iron complex **5** (R=Dur = 2,3,5,6-Me$_4$C$_6$H) and the presumed intermediate complex **6**.
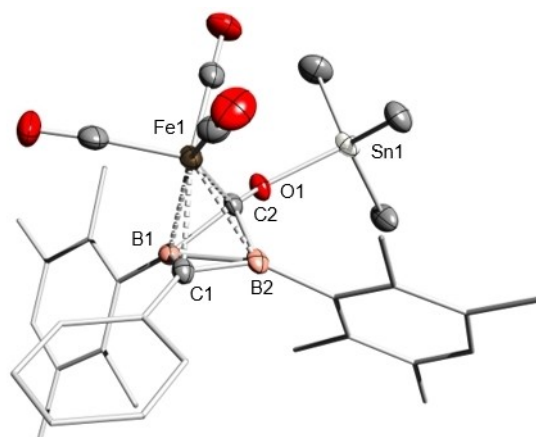
Figure 4. Molecular structure of 1,3-diborete iron complex **5** in the solid state. Thermal ellipsoids at 50% probability. Selected bond lengths [Å] and angles [°]: B1–B2 1.871(5), B1–C1 1.529(4), B2–C1 1.510(4), B1–C2 1.599(4), B2–C2 1.620(4), B1–Fe1 2.210(3), B2–Fe1 2.291(3), C1–Fe1 2.065(3), C2–Fe1 1.906(3) C2–O1 1.318(3); B1–C1–B2 76.0(2), B1–C2–B2 71.1(2).

matches the experimental value reasonably well. The calculated HOMO–LUMO gap is 1.96 eV and thus significantly smaller than for compound **2** and **3**. The computed UV/Vis spectrum consists of a large number of transitions which, taken together, agree well with the experimental spectrum (see SI). The electronic structure, investigated by DFT calculations at the B3LYP/def2tzvpp level of theory, shows the LUMO to be composed of ligand- and metal-centered orbitals (Figure 2).

HOMO and HOMO−2 each show significant overlap between π-electrons, each predominantly located at C1 and C2 and the d orbital at the Fe(CO)$_3$ fragment. HOMO−5 shows orbital overlap of the entire π-system delocalized over the B$_2$C$_2$ centers with the Fe(CO)$_3$ fragment, suggesting a donation in η^4-fashion.

We propose a similar mechanism for the formation of the four-membered ring **5** as for complex **3**. The first step could be the generation of the, albeit undetected, Sn-bridged diborirane complex **6**. The product of oxidative addition of a B–Sn bond to a palladium center was reported by Tanaka and co-workers.[26a] A reason for the instability of the putative intermediate might be the much weaker B–Sn bond, which would facilitate the insertion of either the Fe center or a carbonyl ligand ultimately leading to the 1,3-diborete complex **5**. The free energy of calculated intermediate **6** and free CO is $\Delta G = 21.9$ kcal mol^{-1} higher than that of product **5** (see SI). Alternatively, a π-complex of B=C bond and a Fe(CO)$_4$ fragment without agostic BSn interaction could be envisaged, which, however, is calculated to be $\Delta G = 7.1$ kcal mol^{-1} higher in free energy than compound **6** and free CO (see SI). We did not attempt to compute any of the involved transition states keeping in mind that the unclear nature of the involved Fe$_x$(CO)$_y$ fragments would make this a futile exercise. The preference of this system for the end-on insertion vs. the side-on insertion observed for **3** is ascribed to the pronounced oxophilicity of the SnMe$_3$ group. The apparent kinetic product **5** is calculated to be $\Delta G = 2.0$ kcal mol^{-1} higher in free energy than the hypothetical thermodynamic product, the Me$_3$Sn analogue of **3** (see SI). Heating of **5** above the melting point of 168 °C, however, leads to its decomposition.

As in case of H-bridged diborirane **1**, the uncomplexed Me$_3$Sn-derivative **4** does not react with CO in the absence of iron carbonyls, confirming the involvement of an unknown Fe$_x$(CO)$_y$ species. As a side remark, although numerous reactions of B–Sn reagents with C–C multiple bonds have been reported,[26] the formation of **5** appears to be the first formal borastannylation of a heteronuclear multiple bond.

Conclusion

We have prepared the first diborirane π-complex **2** derived from hydrogen-bridged diborirane **1** and Fe$_2$(CO)$_9$. The Fe(CO)$_3$ fragment is coordinated by the B$_2$C π-system as well as the BH σ-bond so that the non-classical diborirane acts as a 4e$^-$ donor toward the iron center retaining only weak BB interaction. The formal hydroboration of carbon monoxide by non-classical diborirane **2** results in the ring

expansion to an η^5-coordinated B$_2$C$_2$O ligand **3**, although only in the presence of Fe$_2$(CO)$_9$. The particularly strong backdonation from the iron center, which formally turns the 4π-system into a 6π-system, can be seen in the ^{13}C NMR signals of the ring carbon atom as well as in the IR stretching frequencies. In contrast, upon treatment with Fe$_2$(CO)$_9$, the Me$_3$Sn-bridged derivative of **1** is expanded by an end-on inserted CO molecule to yield the η^4-bonded 1,3-diborete complex **5**. The inherent Hückel aromaticity of the 1,3-diborete results in almost negligible backdonation from metal to ligand as the ^{13}C NMR signal is hardly affected by the coordination.

Supporting Information

Plots of NMR, UV and IR spectra as well as details of the single crystal x-ray diffractions studies and DFT-calculations are available in the Supporting Information of this article. Deposition numbers 2357653 (for **2**), 2357652 (for **3**), and 2357648 (for **5**) contain the supplementary crystallographic data for this paper. These data are provided free of charge by the joint Cambridge Crystallographic Data Centre and Fachinformations-zentrum Karlsruhe Access Structures service. The authors have cited additional references within the Supporting Information.[30–40]

Conflict of Interest

The authors declare no conflict of interest.

Data Availability Statement

The data that support the findings of this study are available in the supplementary material of this article.

[1] For selected reviews of metal–organic frameworks see: a) V. F. Yusuf, N. I. Malek, S. K. Kailasa, *ACS Omega* **2022**, *7*, 44507–44531; b) H.-C. Zhou, J. R. Long, O. M. Yaghi, *Chem. Rev.* **2012**, *112*, 673–674.

[2] For selected reviews of dye-sensitized solar cells see: a) A. B. Munoz-Garcia, I. Benesperi, G. Boschloo, J. J. Concepcion,

Angew. Chem. Int. Ed. **2024**, *63*, e202415378 (6 of 8)

© 2024 The Authors. Angewandte Chemie International Edition published by Wiley-VCH GmbH

J. H. Delcamp, E. A. Gibson, G. J. Meyer, M. Pavone, H. Pettersson, A. Hagfeldt, M. Freitag, *Chem. Soc. Rev.* **2021**, *21*, 12450–12550; b) A. Hagfeldt, G. Boschloo, L. Sun, L. Kloo, H. Pettersson, *Chem. Rev.* **2010**, *110*, 6595–6663.

[3] For selected reviews of metallopolymers see: a) Y. Yan, J. Zhang, L. Ren, C. Tang, *Chem. Soc. Rev.* **2016**, *45*, 5232–5263; b) Y. Wang, D. Astruc, A. S. Abd-El-Aziz, *Chem. Soc. Rev.* **2019**, *48*, 558–636; c) R. Whitell, I. Manners, *Adv. Mater.* **2007**, *19*, 3439–3468.

[4] For selected examples of boron containing heterocycles see: a) B. Su, R. Kinjo, *Synthesis* **2017**, *49*, 2985–3034; b) U. M. Dzhemilev, L. I. Khusainova, K. S. Ryazanov, L. O. Khafizova, *Russ. Chem. Bull. Int. Ed.* **2021**, *70*, 1851–1892.

[5] a) C.-W. So, D. Watanabe, A. Wakamiya, S. Yamaguchi, *Organometallics* **2008**, *27*, 3496–3501; b) J. He, F. Rauch, M. Finze, T. B. Marder, *Chem. Sci.* **2021**, *12*, 128–147.

[6] For selected examples of bora and boratabenzenes see: a) G. E. Herberich, G. Greiss, H. F. Heil, *Angew. Chem. Int. Ed. Engl.* **1970**, *9*, 805–806; b) G. E. Herberich, H. Ohst, *Chem.* **1986**, *25*, 199–236; c) A. J. Ashe III, P. Shu, *J. Am. Chem. Soc.* **1971**, *93*, 1804–1805; d) G. C. Fu, *Adv. Organomet. Chem.* **2001**, *47*, 101–119.

[7] For selected examples of borepins see: a) A. J. Ashe III, F. J. Drone, C. M. Kausch, J. Kroker, S. M. Al-Taweel, *Pure Appl. Chem.* **1990**, *62*, 513–517; b) A. J. Ashe III, W. Klein, R. Rousseau, *Organometallics* **1993**, *12*, 3225–3231.

[8] H. Goodman, L. Mei, T. L. Gianetti, *Front. Chem.* **2019**, *7*, 1–19.

[9] T. Kupfer, H. Braunschweig, K. Radacki, *Angew. Chem. Int. Ed.* **2015**, *54*, 15084–1508.

[10] a) H. Braunschweig, T. Herbst, D. Rais, F. Seeler, *Angew. Chem. Int. Ed.* **2005**, *44*, 7461–7463; b) H. Braunschweig, T. Herbst, D. Rais, S. Ghosh, T. Kupfer, K. Radacki, A. G. Crawford, R. M. Ward, T. B. Marder, I. Fernández, G. Frenking, *J. Am. Chem. Soc.* **2009**, *131*, 8989–8999.

[11] H. Braunschweig, P. Brenner, R. D. Dewhurst, I. Krummenacher, B. Pfaffinger, A. Vargas, *Nat. Commun.* **2012**, *3*, 872.

[12] H. Braunschweig, R. D. Dewhurst, K. Radacki, C. W. Tate, A. Vargas, *Angew. Chem. Int. Ed.* **2014**, *53*, 6263–6266.

[13] P. Grewelinger, T. Wiesmeier, B. Morgenstern, C. Präsang, D. Scheschkewitz, *Angew. Chem. Int. Ed.* **2023**, *62*, e202308678.

[14] For selected examples see: a) D. Sharmila, B. Mondal, R. Ramalakshmi, S. Kundu, B. Varghese, S. Ghosh, *Chem. Eur. J.* **2015**, *21*, 5074–5083; b) R. Prakash, A. N. Pradhan, M. Jash, S. Kahlal, M. Cordier, T. Roisnel, J.-F. Halet, S. Ghosh, *Inorg. Chem.* **2020**, *59*, 1917–1927; c) A. Wagner, A. Kaifer, H.-J. Himmel, *Chem. Commun.* **2012**, *48*, 5277–5279; d) K. Saha, D. K. Roy, R. D. Dewhurst, S. Ghosh, H. Braunschweig, *Acc. Chem. Res.* **2021**, *54*, 1260–1273; e) Y. C. Tang, A. L. Thompson, S. Aldridge, *J. Am. Chem. Soc.* **2010**, *132*, 10578–10591; f) T. M. Douglas, A. B. Chaplin, A. S. Weller, X. Yang, M. B. Hall, *J. Am. Chem. Soc.* **2009**, *131*, 15440–15456; g) M. Shimoi, S. Nagai, M. Ichikawa, Y. Kawano, K. Katoh, M. Uruichi, H. Ogino, *J. Am. Chem. Soc.* **1999**, *121*, 11704–11712; h) M. P. Mehn, S. D. Brown, T. K. Paine, W. W. Brennessel, C. J. Cramer, J. C. Peters, L. Que Jr, *Dalton Trans.* **2006**, 1347–1351; i) M. Maekawa, C. G. Daniliuc, P. G. Jones, J. Hohenberg, J. Sutter, K. Meyer, M. D. Walter, *J. Inorg. Chem.* **2013**, 4097–4104; j) K. K. Pandey, *Coord. Chem. Rev.* **2009**, *253*, 37–55.

[15] X. Meng, T. P. Fehlner, A. L. Rheingold, *Organometallics* **1990**, *9*, 534–536.

[16] C. Präsang, Y. Sahin, M. Hofmann, G. Geiseler, W. Massa, A. Berndt, *Eur. J. Inorg. Chem.* **2008**, 5046–5055.

[17] A. Gunale, D. Steiner, D. Schweikart, H. Pritzkow, A. Berndt, W. Siebert, *Chem. Eur. J.* **1998**, *4*, 44–52.

[18] H. Braunschweig, Q. Ye, K. Radacki, A. Damme, *Angew. Chem. Int. Ed.* **2012**, *51*, 7839–7842.

[19] Deposition numbers 2357653 (for **2**), 2357652 (for **3**), and 2357648 (for **5**) contain the supplementary crystallographic data for this paper. These data are provided free of charge by the joint Cambridge Crystallographic Data Centre and Fachinformationszentrum Karlsruhe Access Structures service.

[20] J. J. Turner, M. Bühl, *J. Phys. Chem. A* **2018**, *122*, 3497–3505.

[21] For selected reviews on boron containing transition metal complexes see: a) G. J. Irvine, M. J. G. Lesley, T. B. Marder, N. C. Norman, C. R. Rice, E. G. Robins, W. R. Roper, G. R. Whittell, L. J. Wright, *Chem. Rev.* **1998**, *98*, 2685–2722; b) C. W. Allen, D. E. Palmer, *J. Chem. Educ.* **1978**, *55*, 497–500; c) J. T. Goettel, H. Braunschweig, *Coord. Chem. Rev.* **2019**, *380*, 184–200.

[22] a) R. Hettrich, M. Kaschke, H. Wadepohl, W. Weinmann, M. Stephan, H. Pritzkow, I. Hyla-Kryspin, R. Gleiter, *Chem. Eur. J.* **1996**, *2*, 487–494; b) W. Siebert, M. Bochmann, *Angew. Chem. Int. Ed. Engl.* **1977**, *16*, 857–858; c) W. Siebert, D. Büchner, H. Pritzkow, H. Wadepohl, F.-W. Grevels, *Chem. Ber.* **1987**, *120*, 1511–1514.

[23] For selected examples see: a) K. Khumtaveeporn, H. Alper, *Acc. Chem. Res.* **1995**, *28*, 414–422; b) A. Brand, P. Wegener, A. Hepp, W. Uhl, *Organometallics* **2020**, *39*, 1384–1392; c) J.-B. Peng, F.-P. Wu, X.-F. Wu, *Chem. Rev.* **2019**, *119*, 2090–2127.

[24] K. Skoch, C. Chen, C. G. Daniliuc, G. Kehr, G. Erker, *Dalton Trans.* **2022**, *51*, 7695–7704.

[25] G. E. Herberich, W. Boveleth, B. Hessner, D. P. J. Köffer, M. Negele, R. Saive, *J. Organomet. Chem.* **1986**, *308*, 153–166.

[26] a) S. Onozawa, Y. Hatanaka, T. Sakakura, S. Shimada, M. Tanaka, *Organometallics* **1996**, *15*, 5450–5452; b) L. Weber, H. Wartig, H.-G. Stammler, A. Stammler, B. Neumann, *Organometallics* **2000**, *19*, 2891–2895; c) R. R. Singidi, A. M. Kutney, J. C. Gallucci, T. V. RajanBabu, *J. Am. Chem. Soc.* **2010**, *132*, 13078–13087.

[27] M. Hildenbrand, H. Pritzkow, U. Zenneck, W. Siebert, *Angew. Chem. Int. Ed. Engl.* **1984**, *23*, 371–372.

[28] A. Franken, T. D. McGrath, F. G. A. Stone, *Organometallics* **2005**, *24*, 5157–5166.

[29] A. Hermann, F. Fantuzzi, M. Arrowsmith, T. Zorn, I. Krummenacher B Ritschel, K. Radacki, B. Engels, H. Braunschweig, *Angew. Chem. Int. Ed.* **2020**, *59*, 15717–15725.

[30] G. R. Fulmer, A. J. M. Miller, N. H. Sherden, H. E. Gottlieb, A. Nudelman, B. M. Stoltz, J. E. Bercaw, K. I. Goldberg, *Organometallics* **2010**, *29*, 2176–2179.

[31] L. Benco, T. Demuth, J. Hafner, F. Hutschka, H. Toulhoat, *J. Catal.* **2002**, *205*, 147–156.

[32] G. M. Sheldrick, *Acta Crystallogr.* **2015**, *A71*, 3–8.

[33] G. M. Sheldrick, *Acta Crystallogr.* **2015**, *C71*, 3–8.

[34] C. B. Hübschle, G. M. Sheldrick, B. Dittrich, *J. Appl. Crystallogr.* **2011**, *44*, 28–28.

[35] Gaussian 09, Revision A.02, M. J. Frisch, G. W. Trucks, H. B. Schlegel, G. E. Scuseria, M. A. Robb, J. R. Cheeseman, G. Scalmani, V. Barone, G. A. Petersson, H. Nakatsuji, X. Li, M. Caricato, A. Marenich, J. Bloino, B. G. Janesko, R. Gomperts, B. Mennucci, H. P. Hratchian, J. V. Ortiz, A. F. Izmaylov, J. L. Sonnenberg, D. Williams-Young, F. Ding, F. Lipparini, F. Egidi, J. Goings, B. Peng, A. Petrone, T. Henderson, D. Ranasinghe, V. G. Zakrzewski, J. Gao, N. Rega, G. Zheng, W. Liang, M. Hada, M. Ehara, K. Toyota, R. Fukuda, J. Hasegawa, Ishida, M. T. Nakajima, Y. Honda, O. Kitao, H. Nakai, T. Vreven, K. Throssell, J. A. Montgomery Jr, J. E. Peralta, F. Ogliaro, M. Bearpark, J. J. Heyd, E. Brothers, K. N. Kudin, V. N. Staroverov, T. Keith, R. Kobayashi, J. Normand, K. Raghavachari, A. Rendell, J. C. Burant, S. S. Iyengar, J. Tomasi, M. Cossi, J. M. Millam, M. Klene, C. Adamo, R. Cammi, J. W. Ochterski, R. L. Martin, K. Morokuma, O. Farkas, J. B. Foresman, D. J. Fox, Gaussian, Inc., Wallingford CT, **2016**.

[36] a) J. P. Perdew, *Phys. Rev. B* **1986**, *33*, 8822–8824; b) A. D. Becke, *Phys. Rev. A* **1988**, *38*, 3098–3100.

[37] a) A. Schäfer, H. Horn, R. Ahlrichs, *J. Chem. Phys.* **1992**, *97*, 2571–2577; b) A. Schäfer, C. Huber, R. Ahlrichs, *J. Chem. Phys.* **1994**, *100*, 5829–5835; c) F. Weigend, R. Ahlrichs, *Phys. Chem. Chem. Phys.* **2005**, *7*, 3297–3305; d) F. Weigend, *Phys. Chem. Chem. Phys.* **2006**, *8*, 1057–1065.

[38] S. Grimme, J. Antony, S. Ehrlich, H. Krieg, *J. Chem. Phys.* **2010**, *132*, 154104.

[39] Chemcraft - graphical software for visualization of quantum chemistry computations. https://www.chemcraftprog.com.

[40] T. Lu, F. Chen, *J. Comput. Chem.* **2012**, *33*, 580–592.